Steel and Composite Structures, *Vol. 20, No. 6 (2016) 1305-1322*
DOI: http://dx.doi.org/10.12989/scs.2016.20.6.1305

Structural behavior of partially encased composite columns under axial loads

Margot F. Pereira [1a], Silvana De Nardin [*2] and Ana L.H.C. El Debs [1b]

[1] *Department of Structural Engineering, University of Sao Paulo, Sao Carlos, Brazil*
Avenida Trabalhador Saocarlense 400, Centro, São Carlos-SP - CEP: 13.566-590, Brazil
[2] *Department of Civil Engineering, Federal University of Sao Carlos, Sao Carlos, Brazil*
Rodovia Washington Luís, km 235 - SP-310 São Carlos-SP - CEP 13565-905, Brazil

(*Received September 01, 2015, Revised November 27, 2015, Accepted February 16, 2016*)

Abstract. This paper presents the results of experimental and numerical model analyses on partially encased composite columns under concentric loads. The main objective of this study is to evaluate the influence of replacing the conventional longitudinal and transverse steel bars by welded wire mesh on the structural behavior of these members under concentric loads. To achieve these goals experimental tests on four specimens of partially encased composite columns submitted to axial loading were performed and the results were promising in terms of replacing the traditional reinforcement by steel meshes. In addition, a numerical FE model was developed using the software DIANA® with FX+. The experimental results were used to validate the numerical model. Satisfactory agreement between experimental and numerical results was observed in both capacity and deformability of the composite columns. Despite of the simplifying assumptions of perfect bond between steel and concrete, the numerical model adequately represented the columns behavior. A finite element parametric study was performed and parameters including thickness of the steel profile and the concrete and steel strengths were evaluated. The parametrical study results found no significant changes in the partially encased columns behavior due to variations of the steel profile thickness or yield strength. However, significant changes in the post peak behavior were observed when using high strength concrete and these results suggest a change in the failure mode.

Keywords: partially encased composite column; axial loads; experimental analysis; numerical model; concentric load

1. Introduction

Partially encased composite columns are composite members consisting of a steel profile usually not subjected to local buckling with concrete infill cast between the flanges. In the present study, the cross-section of the composite member is a built-up three-plate steel section combined with high-strength concrete between the flanges (Fig. 1(a)). This type of composite column takes advantages of in-plant prefabrication and efficient compressive load capacity. In addition, partially encased composite members have the fire resistance inherent in a concrete column and the speed

∗Corresponding author, Adjunt Professor, Ph.D., E-mail: snardin@ufscar.br
[a] Ph.D. Student, E-mail: margot.pereira@usp.br
[b] Associate Professor, Ph.D., E-mail: analucia@sc.usp.br

http://www.techno-press.org/?journal=scs&subpage=6 ISSN: 1229-9367 (Print), 1598-6233 (Online)

of erection for a steel structure (Vincent and Tremblay 2001). Firstly, these composite members were investigated by means of composite behavior and concrete infill flanges contribution (Hunaiti and Fattah 1994). Partially encased column specimens subjected to eccentric load and tested under minor axis bending exhibited composite action even without mechanical shear connectors (Hunaiti and Fattah 1994). Contribution of the concrete between the flanges on local and postlocal buckling of composite cross section was investigated and results showed the initial local buckling load is enhanced allowing very slender steel plates to be used in partially encased composite columns (Uy 2001).

Studies with partially encased composite columns have been conducted on a innovative solution developed and patented during the 1990s by the *Canam Manac Inc*. *Company* where the hot-rolled wide flange H steel section had been replaced by a thin-walled welded H-shaped (Fig. 1(b)). This provides an economical solution for steel structures, especially medium-rise and high-rise buildings that support predominantly gravity loads, while other structural elements were responsible for resisting lateral loads (Vincent and Tremblay 2001, Chicoine *et al*. 2002a). The thinner plates had the merit of further material saving and structural weight reduction. However thin plates with large width-to-thickness ratios are very sensitive to local buckling of the flanges. Experimental and numerical studies found that transverse links equally spaced between the flanges and welded along the height of the column provides a very effective way to give lateral support to the free borders of the plates and to reduce the local buckling effects (Tremblay *et al*. 1998, 2002, Cheng *et al*. 2010, Vincent and Tremblay 2001, Chicoine *et al*. 2002a, b, Begum *et al*. 2007). Moreover, the transverse links also provided some confinement to the concrete between the flanges. The effect of parameters such as spacing, size and shape of the links were also studied and a theoretical model to predict the axial capacity of partially encased non-compact columns were proposed and validated by comparing with experimental results (Tremblay *et al*. 2002). Effects of carrying construction loads and confinement and creep of the concrete on the axial load capacity were examined by some researchers and test results suggests that neither the loading sequence nor the creep and shrinkage of the concrete had a significant effect on the ultimate load and failure mode of the tested columns (Tremblay *et al*. 2002, Chicoine *et al*. 2003).

The use of high strength concrete and addition of steel fibers in partially encased members made of thin plates with transversal links welded between opposing flanges were investigated using specimens under concentric and eccentric compressive loads (Prickett and Driver 2006). Experimental results indicate members with high strength present full composite behavior however has a more brittle failure mode than those with normal strength concrete. This brittle failure mode observed in tests was improved with closer transversal links spacing or the addition of steel fibers to the high-strength concrete (Prickett and Driver 2006).

The effects of high strength concrete on the behavior and load capacity of partially encased composite columns was also investigated by Begum *et al*. (2013). In the study, a finite element model including a constitutive model that has the capability to predicting the overall stress-strain of high strength concrete, the post-peak softening branch and the residual strength of steel was developed and validated by comparison with experimental results. The parametric study investigated the influence of the high strength concrete in combination with other parameters such as length-column depth ratio, eccentricity-to-column depth ratio, flange slenderness ratio and transversal link spacing-to-column depth ratio. Numerical results concluded that the influence of the tested parameters is greatly increased by the use of high strength instead of normal strength (Begum *et al*. 2013). Similar to observations of Prickett and Driver (2006), Begum *et al*. (2013) also observed the load-deformation response of columns with high strength concrete exhibited a

(a) Standard cross section (b) Modified cross section

Fig. 1 Cross section of partially encased composite columns

more brittle failure as compared to the normal strength.

The combination of high strength concrete and high strength steel in partially encased columns under eccentric axial loads was investigated by Kim *et al*. (2012) to study the load-carrying capacity and the deformation capacity. Test results showed the load-carrying capacity was limited by the early crushing of concrete due to the inadequate lateral confinement of this material.

Partially encased composite columns under eccentric axial loading producing bending in strong and weak-axis directions were also studied in non-compact steel sections with transversal links (Oh *et al*. 2006). Experimental results of axial force-bending moment capacity of the columns were compared with the predictions of various design code previsions. Although non-compact steel sections presented local buckling and the design codes do not take in account this phenomenon. The EC 4 (2004) code provision was adequate to evaluate the axial-bending capacity of the partially encased under eccentric loads (Oh *et al*. 2006). In the ABNT NBR 8800 (2008), the Brazilian Standard Code of composite structures, local buckling also is not taken in account in the design procedure and the breadth-to-thickness ratio of the flange must be respected for the procedure application. Moreover, partially encased columns require the use of longitudinal and transversal reinforcement bars, especially to prevent cracking and splitting of concrete, which also contribute to the structural safety under fire conditions (ABNT NBR 8800 2008, CEN 2004).

The structural behavior of slender partially encased columns was also investigated and the experimental results were used to calibrate a numerical model to describe the load versus deflection response and develop a parametric study (Ali and Begum 2011). Ali and Begum (2011) concluded the axial capacity of composite columns decrease significantly as the overall column slenderness ratio and load eccentricity ratio increase, especially for columns with thinner steel plates. These experimental and numerical results helped Ali and Begum (2013) in the attempt to represent the axial load and moment capacity by interaction diagrams. Begum and Gosh (2014) proposed the replacement of the steel-concrete composite section by an equivalent steel section which can be easily incorporated in the design and analysis software. Simulation results showed the proposed methodology had good accuracy to predict the behavior and load capacity of partially encased columns under concentric loads.

The behavior of shear walls including partially encased composite columns with cross-section similar to those proposed by Tremblay *et al*. (1998) was investigated by Dastfan and Driver (2015). Experimental results indicated that the detailing of the composite columns played an important role in improving the seismic performance of the specimen.

A summary of the main conclusions based on several experimental and numerical studies with partially encased composite columns is given bellow:

(1) The studies on partially encased composite columns are recent and must be expanded, since some geometrical limits considered may restrict their practical use;
(2) Standard codes to predict the load capacity of partially encased sections limit the width-thickness ratio of the plates of steel profile to avoid the occurrence of local buckling. However, the use of thinner plates may reduce the consumption of steel, hence, the overall cost of the column;
(3) The failure mode of partially encased composite columns with thinner plates consists mostly of concrete crushing combined with local buckling of the steel plates. However, the use of transversal links between the flanges, high-strength concrete or longitudinal and transverse reinforcing bars may change the behavior and load capacity of the composite columns;
(4) Both cross sections, made of thinner plates or compact profiles, showed steel-concrete composite action with or without longitudinal reinforcing bars.

In Brazil, most of the experimental and numerical studies on composite columns were about concrete filled composite columns (De Nardin and El Debs 2007). Therefore, the present study represents the first Brazilian tests on partially encased composite columns consisting of three steel plates of same thickness welded to form the I-welded section with concrete infill cast between the flanges. The main objective is to investigate the replacement of conventional reinforcing bars (longitudinal and transversal steel bars) by welded wire mesh and evaluate the influence of this replacement to the structural behavior and load capacity of partially encased columns under concentric loads. The choice of the welded wire mesh intends to simplify the constructive procedure and develop a more practical and efficient partially encased column. Brazilian construction is considered an industry with relatively low level of technology and industrialization, having its major importance related only to the high number of workers. Most of the constructions have cast on site reinforced concrete structures, requiring intensive labor of low qualification, and these proposed columns are intended to be an alternative solution. Therefore, although the replacement for wire mesh involves more welding points, this option represents a more industrialized solution, with the entire construction process of the column being developed in the plants. In this way, a speed of the construction process and an increase quality of the structural member can be obtained.

This paper presents the results of a set of experiments on four specimens under concentric loads and results of a numerical FE model calibrated using the experimental results. The numerical model was used afterwards to investigate several aspects of the behavior of partially encased composite column.

2. Experimental program

2.1 Test specimens and mechanical properties of the materials

The experimental program consisted of four specimens representing partially encased columns, where the geometry was kept constant and the main studied parameter was the replacing of the steel bars by welded wire mesh. To evaluate the effective influence of the reinforcement type to the behavior and load capacity of the partially encased column, four specimens, two with steel bars and two with welded wire mesh were tested under concentric loads. Each specimen had a cross section of 125 × 131 mm and a height of 1.0 m. Steel plate with identical nominal thickness of

Table 1 Geometry and material mechanical properties

Specimen	Plate size $b_f \times d \times t$ (mm)	Type of reinforcement	Longitudinal reinforcement (cm^2)	Yield stress of steel bars f_{sk} (kN/cm^2)	Yield stress of steel plate f_{yk} (kN/cm^2)
P1 P1R	125 × 131 × 3.18	Steel bars	2.01	Longitudinal: 56.9 Transversal: 67.4	32.3
P2 P2R		Welded wire mesh	1.68	60.0	32.3

3.18 mm is used to form the web and flanges of the I-welded steel profile (see Table 1 and Fig. 2). In Table 1, specimens referred to with letter "*R*" are replicas, e.g., Specimen P1R was a replica of Specimen P1. Due to the reduced cross section of the specimens there was the possibility of occurrence of concrete micro-defects which could affect the results. So specimen and replica have the same geometry and materials and they were tested aiming the validation of the experimental results.

Specimens P1 and P1R had ordinary reinforcing concrete (rebars) with four longitudinal steel bars of 8 mm diameter and transversal reinforcement of 5 mm diameter with spacing of 95 mm. In Specimens P2 and P2R, the steel bars were replaced by square welded steel wires of 4.2 mm diameter with spacing of 63 mm. The transverse reinforcements (steel bars and steel mesh) were welded to the steel web faces of the I profile. The longitudinal area in specimens with welded wire

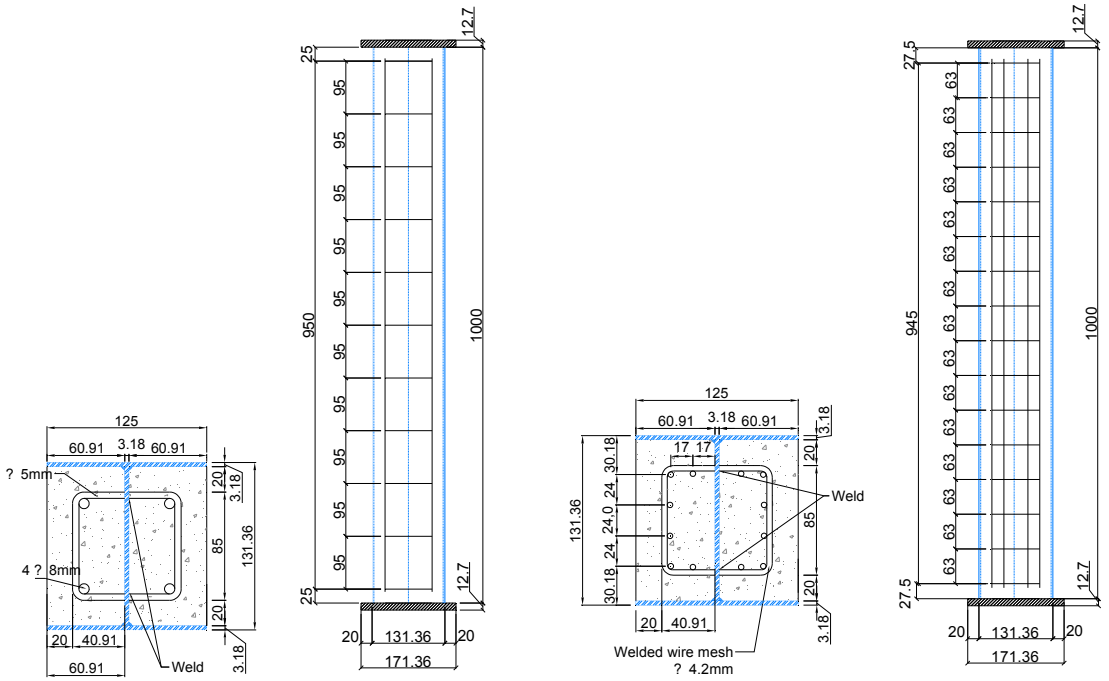

(a) P1 and P1R specimens (b) P2 and P2R specimens

Fig. 2 Geometrical characteristics of specimens (Units: mm)

mesh was 16.4% lower than specimens with ordinary rebars (see Table 1). This had a direct effect on the load capacity of the specimens with welded wire mesh that presented lower peak load than the specimens with rebars (see Table 2).

Although the transverse bars are closer in the steel mesh (63 mm) than in the rebars (95 mm), the amount of transverse reinforcements is the same in both tested situations (equal to 2.2 cm^2). Apparently, the confinement effect of the concrete is predominantly offered by the steel flanges and, therefore, the transverse reinforcing ratio is not the most important parameter in the present study.

Steel end plates 12.7 mm thick were welded at the top and bottom of each specimen for a more uniform load introduction and distribution in the composite column.

All specimens were cast and cured horizontally to reproduce the conditions of a prefabricated composite structural member. At first, one side was cast and a vibrating table was used for adequate fresh concrete consolidation. After a curing period of 4 days, the same procedure was repeated for the second side of the specimen. This procedure eliminates the use of formwork during the concrete cast of the composite columns.

According to the Brazilian code ABNT NBR 8800 (2008), the maximum value specified to the effective width-thickness ratio of the flange, $1.4(E_s/f_y)^{1/2}$, is 34.84, slightly less than flange slenderness ratio, b_f/t, of the tested specimens (b_f/t = 125/3.18 = 39.3). EC 4 (2004) specifies the maximum value of width-thickness ratio of the flange, $44(235/f_y)^{1/2}$, or 37.53. That also is slightly less than the value of the tested specimens. Therefore, considering Brazilian code ABNT NBR 8800 (2008) and CEN (2004), the width-thickness ratio value of the tested specimens was higher than limits recommended by the standard codes and the tests may have been influenced by the local buckling of the flange. The effective width to thickness ratio of the flange was not chosen to avoid local bucking and the dimensions were defined to produce a column that could represent a real column but small enough to be easily tested. As the main objective of the study was to show the viability of the solution with the welded mesh, local buckling could occur in the tests.

The value of elasticity modulus (E_s) was taken equal to 20,000 kN/cm^2 (ABNT NBR 8800 2008) and the concrete infill was normal weight concrete of 55 MPa (f_c = 5.5 kN/cm^2).

Mechanical properties of the concrete and steel were measured experimentally and the average values are presented in Table 1. The yield strength and ultimate strength were measured using three coupons cut from the steel plate and tested according to ASTM A370 (2005). The

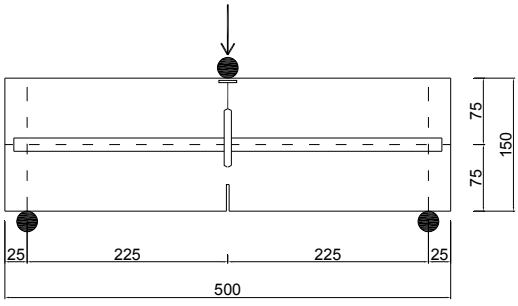

(a) Geometry of sample and load arrangement

(b) Test set up

Fig. 3 Test to tensile fracture energy evaluation (Units: mm)

mechanical properties of the concrete infill were determined using compression tests on ϕ 100 × 200 mm cylinders and the compressive strength were measured on the day of testing. A total of six cylindrical samples, (three of each cast side of the column) were manufactured according to the ABNT NBR 5738 (1994).

In addition, the tensile fracture energy was also evaluated experimentally by bending tests using rectangular samples of 150 × 150 × 500 mm (see Fig. 3). The values measured in this test were used in the development of the FE model.

2.2 Test setup and measurement system

All specimens were tested under concentric compressive loading until failure. Prior to the testing of each specimen, the measurement system was checked with the application of 30% of the predicted ultimate load. Tests were performed with a servo-controlled INSTRON Universal

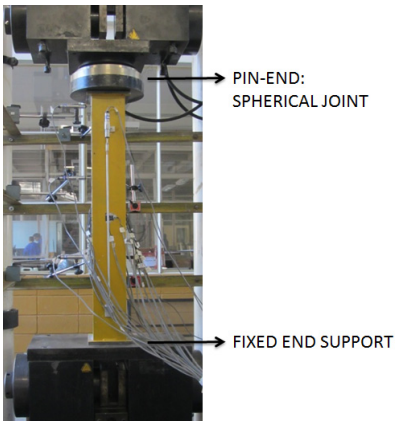

Fig. 4 General layout of test setup

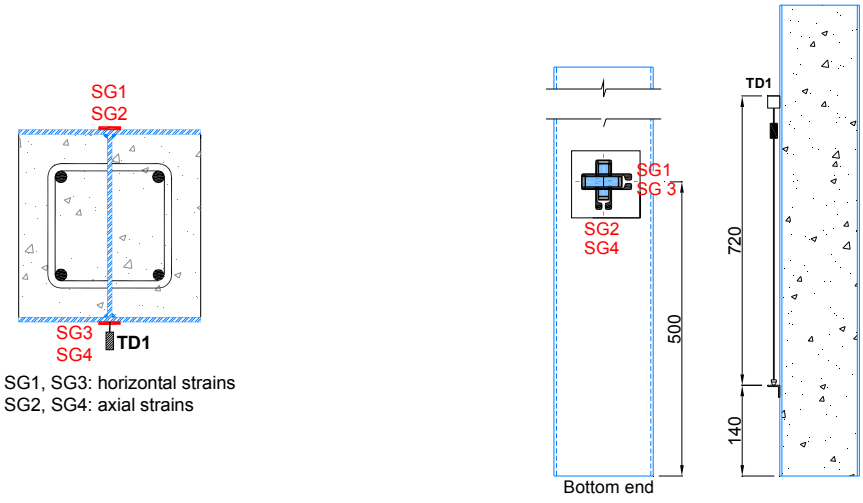

(a) Cross section (b) Along the height

Fig. 5 Arrangement of strain gages and displacement transducer

Testing Machine model 8506 with 2500 kN static loading capacity. Axial loading at a speed of 0.005 mm/s was applied to the specimens by the spherical joint of the Universal Testing Machine. The columns were tested with hinged end at the top and with fixed support at the bottom (Fig. 4).

During the tests, the axial shortening of the specimens was measured by a displacement transducer placed vertically and indicated by T1 in Fig. 5. The strains in horizontal and vertical directions were recorded with strain gauges located on the external face of the flanges of the steel profile, at mid-height of the specimen (at 500 mm of the bottom) - Fig. 5(b).

2.3 Experimental results

2.3.1 Observations and failure load

Fig. 6 presents a general view of the final configuration of the tested specimens. Specimens with conventional reinforced concrete (P1 and P1R), the first signs of local buckling of the steel flanges were observed before the peak load at approximately 0.55 of F_{exp}, however, it was not a determining factor for the failure of these specimens (Fig. 6(a)). A similar behavior was observed for specimens with welded wire mesh (P2 and P2R, Fig. 6(b)). After the peak load had been reached, local buckling was intensified in all specimens with conventional steel bars and welded wire mesh. Therefore, replacing of the conventional steel bars by welded wire mesh showed no significant influence on the failure mode and on the cracks pattern of the concrete infill the flanges. The failure in all specimens was caused by the progressive crushing of the concrete, and the yielding of steel flanges next to it (Fig. 6), which resulted in a very ductile behavior before and after the peak load. However, the cracking pattern was less intense in specimens with welded wire mesh (P2 and P2R) than for those with ordinary reinforcement (P1 and P1R). Although the local buckling of the steel flanges had been observed in all specimens before the peak load, it was not predominant to the failure mode.

The influence of replacing reinforcing bars by welded wire mesh can be evaluated by the peak loads values (F_{exp}, Table 2) and failure modes. The test values of load were compared with those

(a) Specimen P1 (b) Specimen P1R (c) Specimen P2 (d) Specimen P2R

Fig. 6 Final configuration of tested specimens: (a) Specimens with conventional bars; (b) Specimens with welded wire mesh

Table 2 Comparison of experimental, numerical and theoretical values of peak axial load (kN)

Specimen	F_{exp} (kN)	F_{num} (kN)	F_{design} (kN)	F_{num} / F_{exp}	F_{design} / F_{exp}
P1	943.0	971.0	1001.3	1.030	1.062
P1R	974.0			0.997	1.028
P2	954.0	948.3	967.6	0.994	1.014
P2R	950.0			0.998	1.018

obtained on the finite element analysis (F_{num}, Table 2) and calculated using the Brazilian code ABNT NBR 8800 (2008) - (F_{design}, Table 2).

Similar to CEN (2004), the Brazilian code ABNT NBR 8800 (2008) provides two methods for calculation of the resistance of composite columns. The simplified method adopted in the present study makes use of a buckling curve for steel columns implicitly taking account of imperfections. The application of the simplified method is limited to bisymmetric cross-section which does not vary with height, and the local buckling of steel members must be prevented as this phenomenon is not taken account in this procedure. The plastic resistance to axial forces ($N_{pl,Rd}$) is calculated including the individual resistances of the steel profile, the concrete filling and the reinforcement. After applying a reduction factor that takes into account the buckling, a curve given in terms of the slenderness is used to consider the overall bucking. Finally, the design value of the compressive resistance of the column under concentric load is estimated (F_{design}, Table 2).

As mentioned in item 2.1, local buckling could occur during the tests because the width to thickness ratio of the plates was slightly higher than the standard limits. In fact, this phenomenon was observed during the tests but apparently it was not significant for the failure mode and load capacity of the tested columns, since a very good agreement was found between experimental and design values (F_{design}) of the peak load (F_{exp}).

Comparing the specimens with conventional reinforced concrete, the mean value of the design-to-experimental peak load ratio, F_{design}/F_{exp}, is 1.04. For specimens with welded wire mesh the mean value of the F_{design}/F_{exp} ratio is 1.02. These values indicate the excellent prediction of the ultimate capacity of partially encased columns under concentric loads by the Brazilian code ABNT NBR 8800 (2008).

These results indicate that although local buckling is a failure mode not accounted for Brazilian code, these standard procedure can be used to predicting the load capacity in these cases because local buckling was not the predominant failure mode.

2.3.2 Load vs. strains behavior

The load-axial shortening behavior provides information on the maximum load and apparent ductility of each tested specimen. The influence of the type of reinforcement on the global response of the tested specimens can be evaluated by the axial strains (Fig. 7). The latter corresponds to the average shortening of the specimen measured by a longitudinal transducer displacement (TD1, Fig. 5), divided by the length between the attachment points (720 mm). The applied load was divided by the peak load (load/F_{exp}) of each tested specimen shown in Table 2. Specimen P1 and the P1R replica presented very similar behavior (Fig. 7(a)) and the same was observed for specimens with welded wire mesh (P2 and P2R, Fig. 7(b)). The average curves are shown in Fig. 7(c). The behavior of Specimens P1 and P1R was almost linear until approximately load/peak load ratio of 55% (Fig. 7(a)). The same behavior almost linear until $0.55F_{exp}$ was

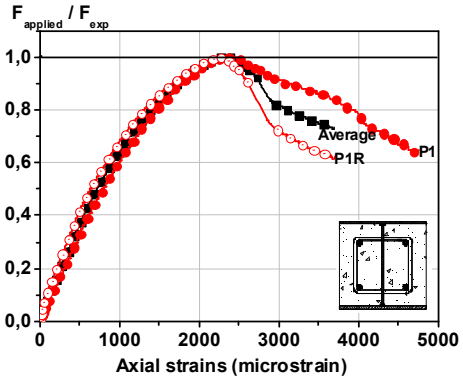

(a) Specimen with conventional steel bars

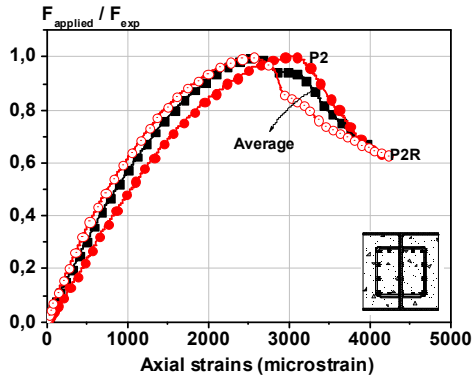

(b) Specimens with welded steel wire

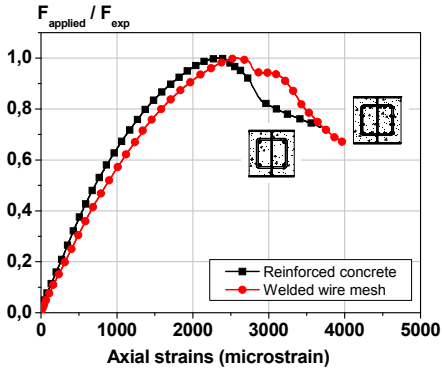

(c) All tested specimens

Fig. 7 Load/peak load ratio vs. Axial strains experimental curves

recorded from specimens with welded wire mesh (P2 and P2R, Fig. 7(b)). However Specimen P2R (replica) showed lower stiffness since the first stages of loading including the linear phase. After $0.55F_{exp}$, the stiffness started to decrease due to the local buckling of the steel flanges and crushing of the concrete (Figs. 7(c)). The influence of the reinforcement type on the behavior of the composite columns can be observed in Fig. 7(c) and these curves indicate that the specimens with conventional steel bars are slightly stiffener in the first stages of loading, however similar behavior was observed in the post-peak branch.

The peak load of specimens with conventional reinforced concrete were recorded at 2341 microstrain, whereas the average value in specimens with welded wire mesh was 2799 microstrain, confirming these specimens are more deformable than specimens with conventional steel bars.

2.3.3 Strains in the steel profile

Longitudinal strains were recorded in all specimens with strain gauges located on the flanges of the steel profile (mid-height region of the specimen) and the average values are shown in Fig. 8. The strains of specimens and replicas were very similar for both, conventional reinforcing concrete and welded wire mesh specimens. The axial strain values recorded on flanges of all tested specimens were also very similar in all stages of loading, in pre-peak branch. Only specimen P1, with ordinary reinforcing bars, exhibited a softer behavior and higher values of axial strains in the

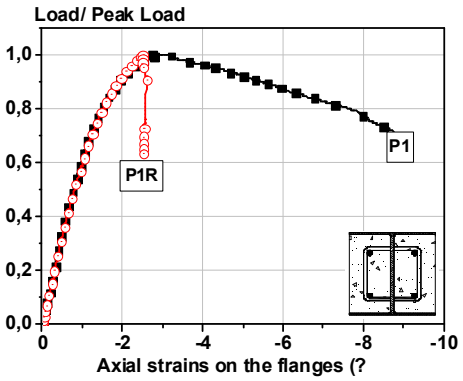

(a) Specimen with conventional steel bars

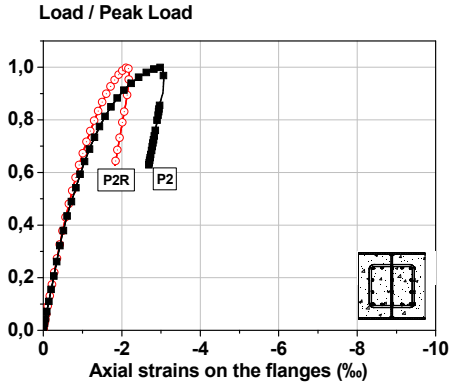

(b) Specimens with welded steel wire

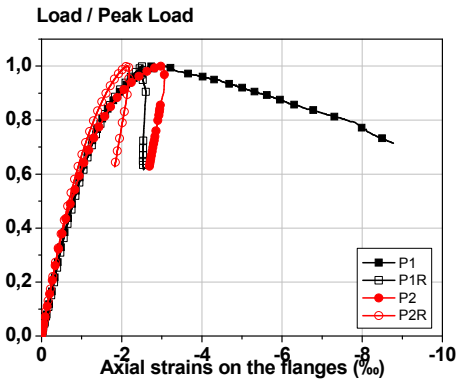

(c) All tested specimens

Fig. 8 Axial strains on steel flanges

post peak stage. That suggests the steel yielding was primarily responsible for the load capacity and ductility in the post-peak branch.

However, local buckling occurred near the location of the strain gauges. This could have damaged the strain gauges. Except for specimen P1, the influence of the reinforcement type was not significant for the values and behavior of the axial strains of the steel profile flanges (Fig. 8(c)).

3. Numerical analysis

3.1 Description of the numerical model

The numerical analysis was conducted with the objective of developing the simplest possible model, which could represent the behaviour and load capacity of partially encased columns under concentric loads. Local bucking was not taken into account in the present study. The finite element model of the composite column was developed using the Fx+ DIANA® version v. 9.4.4, finite element code, by means of a three-dimensional model of geometrical characteristics identical to the experimental specimens. The numerical model was used to represent the behavior of partially encased columns under concentric load and to evaluate the effects of parameters such as compressive strength of concrete, thickness of the steel plate and the yield stress of the steel on the

behavior and load capacity. The 3-D HX24L solid finite elements available in the finite elements library of DIANA® was selected to model the components of the composite member. The 3-D HX24L is an isoparametric element with eight nodes, three translational degrees of freedom at each node and linear approximation of displacements. Fig. 9 shows a general view of the finite element mesh, as well as the components of the numerical model, namely steel profile (Fig. 9(b)), longitudinal and transverse reinforcing bars (Fig. 9(c)) and concrete infill (Fig. 9(d)). The mesh was refined in the load introduction region and a rigid plate was used for application of compressive load to avoid stress concentration. Steel bars embedded in solid elements representing the concrete were used to represent the reinforcing bars of composite column in the numerical model. Therefore, in the numerical model, reinforcement bars are represented by lines. The main differences between P1and P2 were the number and position of the lines representing the steel bars. Specimen P1 was modelled with only four longitudinal lines (bars), whereas P2 column had 12 longitudinal bars representing the welded wire mesh (see more details in Fig. 2).

The compressive load was applied to a rigid plate (elasticity modulus of 1000 GPa) that was placed on the upper end of the column, where the load was applied in the form of prescribed displacements. The imperfections of the plates were represented by an accidental eccentricity of the compressive load considered in the numerical modelling. Accidental eccentricity value adopted was 4.5 mm in the x-axis direction. In an attempt to reproduce the boundary conditions of the experimental test, translations in z direction were restricted on all bottom nodes and translations in x and y directions were restricted at the bottom only for the nodes of the web of the steel profile.

Non-linear constitutive relationships for concrete and steel were assumed in the FE model considering homogeneous materials and with isotropic behavior. The steel material properties of the steel plates and reinforcing bars are simulated by a bilinear stress-strain response and elastic

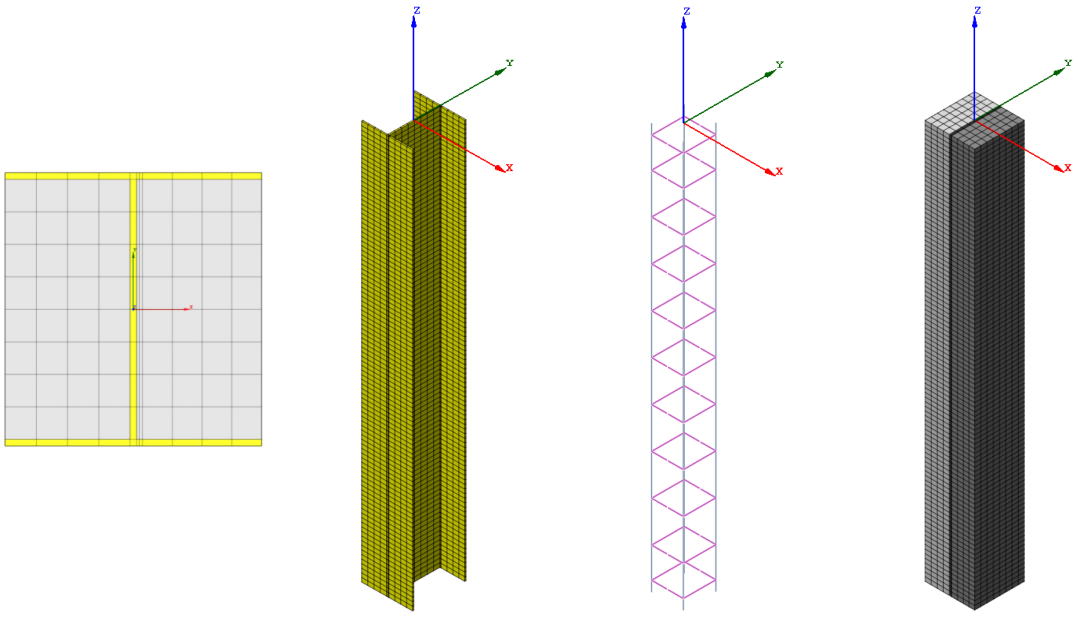

(a) Cross section (b) Steel profile (c) Reinforcing bars (d) Concrete infill flanges

Fig. 9 Components of the numerical model

perfectly-plastic behavior, with Von Mises plasticity criterion, using the measured values of yield strength shown in Table 1. The elasticity modulus of both, steel plates and reinforcing bars was taken equal to 20,000 kN/cm^2. The value of Poisson's ratio for steel used in the numerical analysis was 0.3.

Smeared crack model was used to simulate the concrete material behavior in the composite column. This constitutive model is based on total strain and the stress is described as a function of strain. In the fixed stress-strain concept, a fixed coordinated system is used in the evaluation of the stress-strain relationships and it is defined upon cracking. (Diana Manual 2014). The input for total strain crack models on DIANA® consists of the basic properties (elasticity modulus and Poisson's ratio, for instance) and the properties of the post-peak behavior in tension, shear and compression. The post-cracking and post-crushing properties were modelled using softening functions based on fracture energy. An exponential curve is used to represent the softening of the material under tension and a parabolic curve to represent the behavior under compression (Fig. 10). The tensile fracture energy was measured in the test to fracture energy evaluation and the found value was 0.17 N/mm (Fig. 3). On the other hand, the value of compressive fracture energy was calibrated from the results of the overall structural behavior of the columns and the found value was 1.0 N/mm. The compressive strength, which was measured experimentally by standard tests, had an average value equal to f_c = 5.5 kN/cm^2. The value of tensile strength of concrete was taken equal to 0.409 kN/cm^2 and the value of Poisson´s ratio for concrete used in the numerical analysis was 0.2.

In the numerical analysis, the compressive strength was reduced by a reduction factor taking account of the size of the specimen in relation to the test cylinder of concrete, variation in compaction and curing methods. A similar procedure was suggested by Neville (1995) and Chicoine *et al*. (2002a).

Additional basic assumptions, such as small displacements and deformations and perfect bonding between the concrete and the steel were adopted in the present numerical model. The assumption of no slip between concrete and steel was based on a previous study conducted by authors (Pereira 2014) where linear steel-concrete interfaces were developed to evaluate if a simplified procedure would be enough to represent the experimental behavior. The results of numerical study showed no significant changes in the peak load value and structural behavior when the interface was represented and, therefore, no steel-concrete interfaces were used in numerical models and no relative steel-concrete slip was considered in the FE model.

The solution technique adopted was Quasi-Newton method with convergence criterion based on energy. In this study, the load was applied using displacement control technique with a step of 0.25 mm.

(a) Tensile softening (b) Compression softening

Fig. 10 Softening functions for concrete based on fracture energy

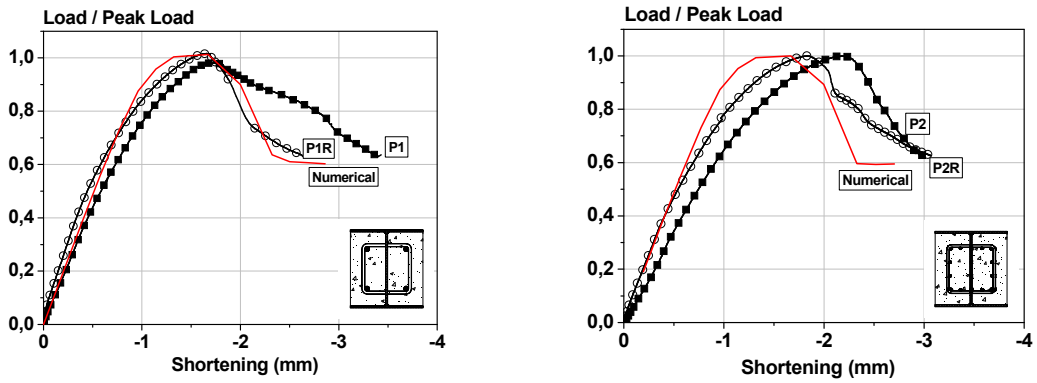

(a) Specimens with conventional reinforced concrete (b) Specimens with welded wire mesh

Fig. 11 Numerical and experimental Load versus Shortening responses

3.2 Results of numerical analyses

3.2.1 Performance of the finite element model

The main objective of the numerical simulation by FE model was the development of an efficient numerical model that simulates the behavior of concentrically loaded partially encased columns. In order to evaluate the performance of the finite element model, the experimental and numerical values of the peak loads (Table 2) and the load-shortening responses were used.

Comparing the specimens with conventional reinforced concrete, the mean value of the numerical-to-experimental peak load ratio, F_{num}/F_{exp}, is 1.013 (Table 2) and this indicates the excellent performance of the numerical model in predicting the ultimate capacity of partially encased columns under concentric loads. In specimens with welded wire mesh, the average numerical-to-experimental peak load ratio, F_{num}/F_{exp}, was 0.996. Therefore, a good agreement for peak load was also observed in these specimens and these results confirm the proposed FE model can be used in predicting the ultimate capacity.

The overall response of composite columns under concentric loads can be evaluated by load-shortening behavior. In Fig. 11, the experimental and numerical responses are compared and both responses are very close indicating an accurate representation of ductility up to the peak load. Therefore, good agreements were observed between the experimental and numerical results for the elastic stiffness and peak load, especially for specimen P1R, for which the post-peak behavior was very well represented by the numerical model. The experimental and numerical Load/Peak vs. Shortening responses the specimens with welded steel wire (P2 and P2R, Fig. 11(b)) were very close, especially at the first stages of loading for specimen P2R. However, the numerical model is observed to underestimate the axial deformation in the pre-peak branch, including the deformation at peak load for specimens with welded steel wire.

Although the numerical model in some cases does not match as well with the experimental curves after the peak, the load capacity can be estimated accurately when the partially encased columns are under concentric loads.

3.2.2 Parametric analysis

A total of twelve concentrically loaded composite column specimens were studied using the FE model developed in the present study. The influence of parameters such as compressive strength of

concrete (f_c), thickness of steel plate of I-profile and yielding stress of steel plates (f_y) on the load capacity and load-shortening responses were evaluated. The values of numerical peak loads (F_{num}) are shown in Table 3.

- *Effect of concrete strength* (f_c)

The compressive concrete strength plays an important role in increasing the load-carrying capacity of composite columns. The load in columns having conventional reinforcing bars and welded wire mesh is plotted against shortening for concrete strengths of 25, 50 and 80 MPa in Fig. 12(a). Similar load-shortening response in the pre-peak stage was observed for specimens with 25 and 50 MPa concretes. On the other hand, composite columns with high strength concrete (80 MPa) presented a significant increase in stiffness in pre-peak branch until the peak load, followed by a sudden loss of load capacity after the peak load is reached (Fig 12(a)). Columns of higher concrete strength showed higher values of column capacity. A sudden loss of stiffness and load capacity in the post-peak branch were observed for all specimens investigated, including conventional reinforced concrete and welded wire mesh. The residual load capacity was more evident in composite columns of lower concrete strengths, as expected due to the higher ductility of these concretes in comparison with higher strength concretes (Fig. 12(a)). The effect of type of reinforcement on the load capacity and response was not significant for the specimens and strength values considered in the present study.

- *Effect of the steel plates thickness*

As expected, increasing the thickness of the steel plates resulted in an increase in the load capacity and stiffness of the composite column (Table 3 and Fig. 12(b)). The load-shortening responses were approximately linear for columns of 3.18 mm and 4.76 mm thickness, respectively until loads of 700 kN and 800 kN. After these values of loads, the responses showed a decrease of stiffness until to the peak load. An almost horizontal post peak branch was observed for both thicknesses and the loss of stiffness occurred at the same vertical shortening value, which indicates the failure mode is related to the crushing of concrete infill. Moreover, the residual load capacity

Table 3 Load peak values obtained from parametric analysis

	Thickness of plates (mm)	Reinforcement	f_{yk} (kN/cm^2)*	f_{ck} (kN/cm^2)*	F_{num} (kN)
Reference values	3.18	Steel bars	32.3	5.0	970.97
		Welded wire mesh			948.33
Effect of concrete strength	3.18	Steel bars	32.3	2.5	757.39
				8.0	1455.00
		Welded wire mesh	32.3	2.5	736.39
				8.0	1457.11
Effect of plate thickness	4.76	Steel bars	32.3	5.0	1112.67
		Welded wire mesh			1099.78
Effect of yielding strength	3.18	Steel bars	69.0	5.0	1424.96
		Welded wire mesh			1403.37

*f_{yk}: yielding strength of steel plates; f_{ck}: compressive strength of concrete

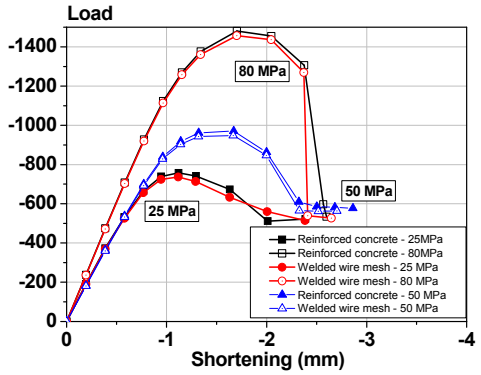

(a) Effect of concrete strength

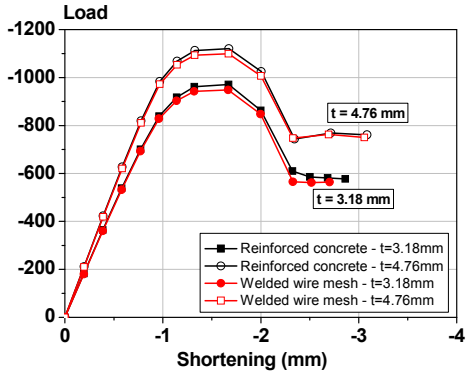

(b) Effect of thickness of steel plate

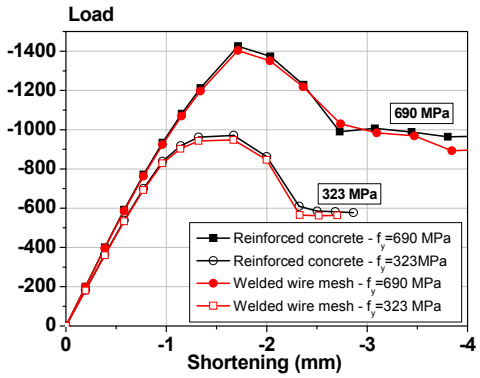

(c) Effect of yielding strength of steel plates

Fig. 12 Load vs. Shortening curves

was higher for the higher thickness, which indicates the yielding of steel plates was responsible for the residual load capacity in the post-peak branch. Therefore, the contribution of the steel profile in the load capacity of the composite column increases with the thickness of plates, also increasing the residual load capacity.

- *Effect of the yield strength of the steel profile*

The influence of the yielding strength of the steel plates on Load vs. Shortening behavior is shown in Fig. 12(c). No significant changes were observed in the pre-peak response when the yielding strength of the steel plates were increased from 323 MPa to 690 MPa. However, the post-peak branch showed changes, including the residual load capacity, which indicates some influence of the yield strength of the steel plates on the branch. The use of higher yield strength produced higher values of peak load. Almost linear responses were observed until 700 kN in specimens with lower yield strength. Whereas in specimens with higher yield strength the linear responses were observed almost until the peak load. The peak load values and responses in both pre and post-peak branches from specimens with conventional reinforced concrete and welded wire mesh were very close (see Fig 12(c)), which indicates no significant influence of the yielding strength and type of reinforcement on the behavior of partially encased columns.

4. Conclusions

This paper addressed experimental and numerical results of a study of partially encased composite columns under concentric loads. Four tests were conducted for the investigation of the effects of types of reinforcement on the load capacity and behavior of the composite columns. According to the short test program outlined and FE model analysis, the following conclusions can be drawn:

- The effect of the type of reinforcement on the load capacity, stiffness and post-peak behavior was not significant and the welded wire mesh can be used to replace the conventional steel bars simplifying of the fabrication procedure. However, these results must be confirmed by new experimental programs for more details on the proposed replacement.
- The numerical model reproduced the experimental response and load capacity of the tested specimens and can be used to investigate the influence of other parameters, such as, compressive strength of concrete, thickness and yield strength of steel plates.
- Numerical results of the parametric analysis showed the increase of the thickness or yield strength of the steel plates affected only the load capacity of the column and caused no significant changes in its structural behavior.
- The structural response of the composite columns under concentric loading was affected only when the concrete strength was increased to 80 MPa, which suggests a change in the failure mode. However, the behavior in the post peak branch for high strength concrete must be confirmed by experimental tests.

Acknowledgments

The authors would like to thank the financial support by grant #2012/07885-5 and grant #2014/12694-0 Sao Paulo State Research Support Foundation (FAPESP).

References

ABNT NBR 5738 (1994), NBR 5738: Concrete - Procedure for molding and curing the coupons, Rio de Janeiro, Brazil. [In Portuguese]

ABNT NBR 8800 (2008), NBR 8800: Design and execution of steel concrete composite building structures: Procedures, Rio de Janeiro, Brazil. [In Portuguese]

Ali, S. and Begum, M. (2011), "Behavior of partially encased slender composite columns in eccentric loading", *Proceedings of the 4th Annual Paper Meet and the 1st Civil Engineering Congress*, Dhaka, Bangladesh, December, pp. 251-260.

Ali, S. and Begum, M. (2013), "Load-moment interaction diagrams of slender partially encased composite columns", *Malay*. *J*. *Civil Eng*., **25**(2), 254-266.

ASTM A370 (2005), ASTM A370: Standard test methods and definitions for mechanical testing of steel products, American Society for Testing and Materials.

Begum, M. and Gosh, D. (2014), "Simulations of PEC columns with equivalent steel section under gravity loading", *Steel Compos*. *Struct*., *Int*. *J*., **16**(3), 305-323.

Begum, M., Driver, R.G. and Elwi, A.E. (2007), "Finite-element modeling of partially encased composite columns using the dynamic explicit method", *J*. *Struct*. *Eng*., **133**(3), 326-334.

Begum, M., Driver, R.G. and Elwi, A.E. (2013), "Behaviour of partially encased composite columns with

high strength concrete", *Eng. Struct.*, **56**, 1718-1727.
CEN (2004), ENV 1994-1-1: Design of composite steel and concrete structures – Part 1-1: General rules and rules for buildings, Brussels, Belgium.
Chen, Y., Wang, T., Yang, J. and Zhao, X. (2010), "Test and numerical simulation of partially encased composite columns subject to axial and cyclic horizontal loads", *Int. J. Steel Struct.*, **10**(4), 385-393.
Chicoine, T., Tremblay, R., Massicotte, B., Ricles, J.M. and Lu, L. (2002a), "Behavior and Strength of partially encased composite columns with built-up shapes", *J. Struct. Eng.*, **128**(3), 279-288.
Chicoine, T., Tremblay, R. and Massicotte, B. (2002b), "Finite element modeling and design of partially encased composite columns", *Steel Compos. Struct.*, *Int. J.*, **2**(3), 171-194.
Chicoine, T., Tremblay, R. and Massicotte, B. (2003), "Long-term behavior and strength of partially encased composite columns made with built-up steel shapes", *J. Struct. Eng.*, **129**(2), 141-150.
Dasfan, M. and Driver, R. (2015), "Large-scale test of a modular steel plate shear wall with partially encased composite columns", *J. Struct. Eng.*, **141**(10), 04015142.
De Nardin, S. and El Debs, A.H.C. (2007), "Shear transfer mechanisms in composite columns: an experimental study", *Steel Compos. Struct.*, *Int. J.*, **7**(5), 377-390.
Diana Manual (2014), DIANA finite element analysis: User's manual release 9, Material library; Delft, The Netherland.
Hunaiti, Y.M. and Fattah, B.A. (1994), "Design considerations of partially composite columns", *Proc. Inst. Civ. Eng., Struct. Build.*, **106**(2), 75-82.
Kim, C-S., Park, H-G., Chung, K-S. and Choi, I-D. (2012), "Eccentric axial load testing for concrete-encased steel columns using 800 MPa steel and 100 MPa concrete", *J. Struct. Eng.*, **138**(8), 1019-1031.
Neville, A.M. (1995), *Properties of Concrete*, (4th Ed.), Wiley, New York, NY, USA.
Oh, M.H., Ju, Y.K., Kim, M.H. and Kim, S.D. (2006), "Structural performance of steel-concrete composite column subjected to axial and flexural loading", *J. Asian Architect. Build. Eng.*, **5**(1), 153-160.
Pereira, M.F. (2014), "Experimental and numerical analysis of partially encased composite columns", Thesis (Master Degree); University of Sao Paulo, Sao Carlos, Brazil. [In Portuguese]
Prickett, B.S. and Driver, R.G. (2006), "Behavior of partially encased columns made with high performance concrete", Structural Engineering Report (n. 262); Department of Civil and Environmental Engineering, University of Alberta, Edmonton, AB, Canada.
Tremblay, R., Massicotte, B., Filion, I. and Maranda, R. (1998), "Experimental study on the behavior of partially encased composite columns made with light welded H steel shapes under compressive axial loads", *Proceedings of Annual Technical Session*, *Structural Stability Research Council*, Atlanta, GA, USA, pp. 195-204.
Tremblay, R., Chicoine, T. and Massicotte, B. (2002), "Design equation for the capacity of partially encased non-columns", *Proceedings of Composite Construction in steel and concrete IV*, ASCE, Reston, VA, USA, pp. 506-517.
Uy, B. (2001), "Local and postlocal buckling of fabricated steel and composite cross sections", *J. Struct. Eng.*, **127**(6), 666-677.
Vincent, R. and Tremblay, R. (2000), "Design and application of partially encased non-compact composite columns for high-rise buildings", *Proceeding of Composite Construction IV*, Banff, AB, Canada, May, pp. 854-864.
Vincent, R. and Tremblay, R. (2001), "An innovative partially composite column system for high-rise buildings", *Proceedings of North American Steel Construction Conference*, Fort Lauderlade, FL, USA.

CC